AD-A067 751 LEE (J S) ASSOCIATES INC ARLINGTON VA F/G 9/1
DETECTION PERFORMANCE OF AN FM CORRELATOR.(U)
MAR 79 J S LEE, L E MILLER N00014-77-C-0056
UNCLASSIFIED JTR-79-03 NL

1 OF 1
ADA
067751

END
DATE
FILMED
6-79
DDC

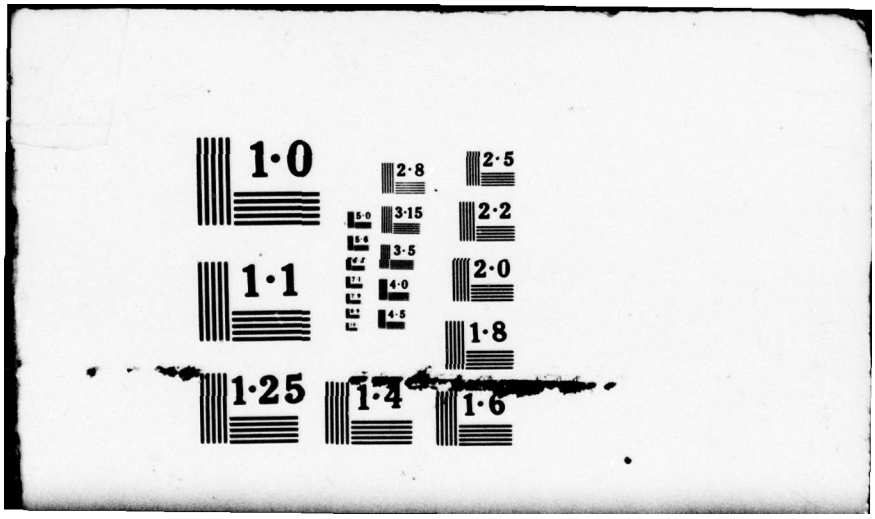
1·0
1·1
1·25
2·8
3·15
3·5
4·0
4·5
1·4
2·5
2·2
2·0
1·8
1·6

LEVEL II

(12)

L. S. LEE ASSOCIATES, INC.

LEVEL II

(12)

DETECTION PERFORMANCE OF AN FM CORRELATOR

by

J. S. Lee

L. E. Miller

JTR-79-03
March 1979

Prepared for:

The Office of Naval Research
Statistics and Probability Program

Under Contract N00014-77-C-0056

Prepared by:

J. S. LEE ASSOCIATES, INC.
2001 Jefferson Davis Highway
Suite 201, Crystal Plaza One
Arlington, Virginia 22202
(703) 979-2230

UNCLASSIFIED

SECURITY CLASSIFICATION OF THIS PAGE (When Data Entered)

REPORT DOCUMENTATION PAGE

READ INSTRUCTIONS BEFORE COMPLETING FORM

1. REPORT NUMBER

2. GOVT ACCESSION NO.

3. RECIPIENT'S CATALOG NUMBER

4. TITLE (and Subtitle)

(6) Detection Performance of an FM Correlator.

5. TYPE OF REPORT & PERIOD COVERED

Feb. 1, 1978 -- Jan. 31, 1979

6. PERFORMING ORG. REPORT NUMBER

(14) JTR-79-03

7. AUTHOR(s)

(10) J. S. Lee, L. E. Miller

8. CONTRACT OR GRANT NUMBER(s)

(15) N00014-77-C-0056

9. PERFORMING ORGANIZATION NAME AND ADDRESS

J. S. LEE ASSOCIATES, INC.
2001 Jefferson Davis Highway
Arlington, Virginia 22202

10. PROGRAM ELEMENT, PROJECT, TASK AREA & WORK UNIT NUMBERS

11. CONTROLLING OFFICE NAME AND ADDRESS

Statistics and Probability Program
Office of Naval Research
Arlington, Virginia 22217

(11)

12. REPORT DATE

March 1979

13. NUMBER OF PAGES

44 + iii

14. MONITORING AGENCY NAME & ADDRESS (if different from Controlling Office)

(9) Rept. for 1 Feb 78-31 Jan 79,

(12) 48p.

15. SECURITY CLASS. (of this report)

UNCLASSIFIED

15a. DECLASSIFICATION/DOWNGRADING SCHEDULE

16. DISTRIBUTION STATEMENT (of this Report)

Approved for public release; distribution unlimited

17. DISTRIBUTION STATEMENT (of the abstract entered in Block 20, if different from Report)

18. SUPPLEMENTARY NOTES

19. KEY WORDS (Continue on reverse side if necessary and identify by block number)

Frequency modulation, detection, FM correlator, false alarm rate, detection probability

20. ABSTRACT (Continue on reverse side if necessary and identify by block number)

Detection of a carrier frequency-modulated by a Gaussian random process is studied for a detector consisting of the filtered product of two FM limiter/discriminator outputs. Results show that high detection probabilities can be achieved for appropriate values of receiver parameters.

DD FORM 1 JAN 73 1473 EDITION OF 1 NOV 65 IS OBSOLETE

393 892

UNCLASSIFIED LB

SECURITY CLASSIFICATION OF THIS PAGE (When Data Entered)

DETECTION PERFORMANCE OF AN FM CORRELATOR

Table of Contents

DETECTION PERFORMANCE OF AN FM CORRELATOR

I. Introduction

A. Background. Developing the capability to detect and track signal energy contained in selected narrow spectral windows continues to be a significant challenge to the undersea warfare community. Potential targets can be characterized acoustically by spectra featuring one or more narrowband emissions of uncertain or random bandwidth, whose center frequencies are subject to doppler shifting as the targets move. Therefore, detection of such emissions and estimation of their frequencies as they vary in time (tracking) allow both target identification and localization. In many ways the dynamic behavior of these emissions resembles conventional frequency modulation.

The methods presently employed in spectral estimation for the purpose of detecting and tracking undersea targets for the most part are based on computation of discrete Fourier transforms (DFT). In some applications, these methods are not practical from the point of view of complexity and cost. For example, the design of an expendable sensor array is usually constrained by a cost figure, and thus it is desirable to use a spectral estimation scheme which is inherently simple and relatively inexpensive.

The investigation reported herein is aimed at evaluating alternate methods proposed for spectral detection and estimation which do not require DFT processing. Representative of these methods is the FM correlator illustrated in Figure 1, in which waveforms from two sensors with the same spectral band (or in two spectral bands from the same sensor) are each processed as if they were FM signals, and the results correlated.

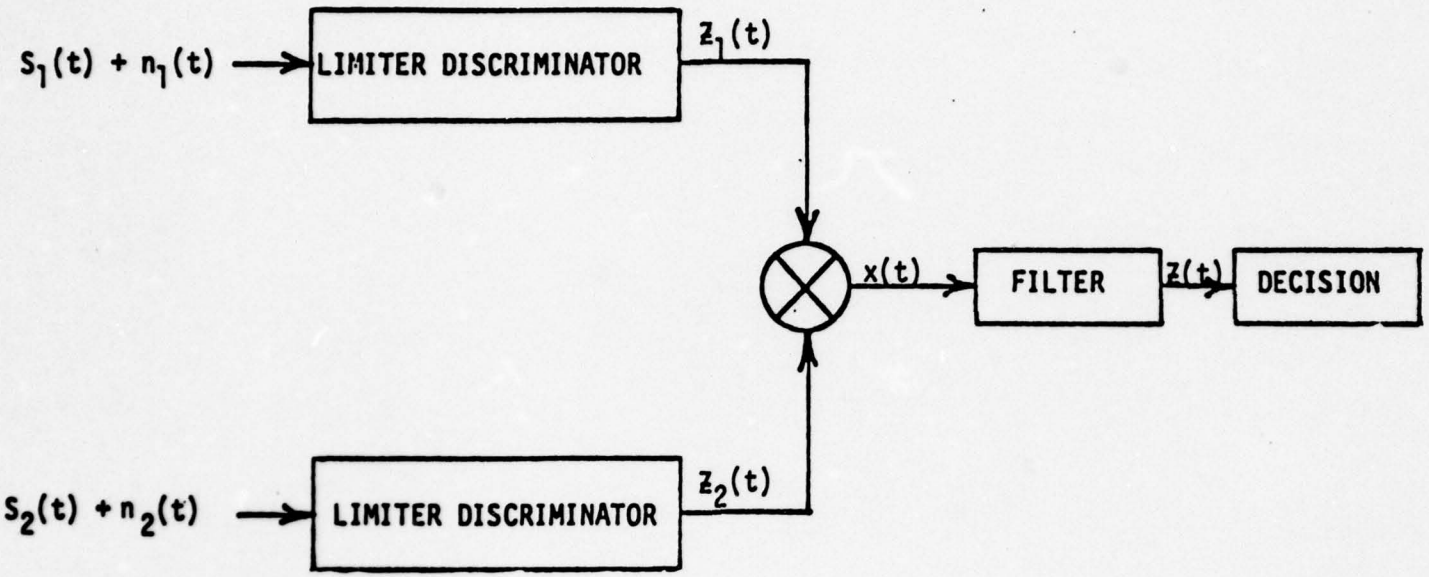

FIGURE 1 FM CORRELATOR MODEL

The FM detectors depicted in the diagram are assumed to be conventional employing a limiter and a discriminator such as the Travis type shown in Figure 2. Use of an integrated circuit version would also be in harmony with the analysis employed, since the modelling is based on the idea of frequency-to-amplitude conversion in which the multiplier inputs z_1 and z_2 are, over a given bandwidth, linear functions of the instantaneous frequencies of the inputs to the two channels. For convenience, the conversion is understood to be

$$\left.\begin{aligned} z_i(t) &= g_i[\omega_i(t)] \\ &= \omega_i(t) - \omega_o \\ &= \Delta\omega_i(t) \end{aligned}\right\} \quad \begin{aligned} &i = 1, 2 \\ &|\omega_i - \omega_o| < W/2. \end{aligned}$$

Thus the correlator filter output at time T is

$$z(T) = \int_0^T dt\; z_1(T - t)z_2(T - t)h(t)$$

$$= \int_0^T dt\; \Delta\omega_1(T - t)\Delta\omega_2(T - t)h(t),$$

an estimate of the cross-correlation between the frequencies in the two channels. When a target is present, the output of the multiplier is

$$(\Delta\omega_s + \Delta\omega_{n_1})(\Delta\omega_s + \Delta\omega_{n_2})$$

$$= (\Delta\omega_s)^2 + \text{noise}$$

and the correlator provides a smoothed estimate of the mean square target frequency deviation from the center of the band when the relative time delay between the channels has been compensated for.

The present effort is intended to prove the concept of detection using an FM correlator with quantitative results. Numerical results presented assume that the relative time delay between the target waveforms received in the two channels has been removed, although in the analysis and in computer programs this delay can be specified as a parameter. Also, in the present analysis

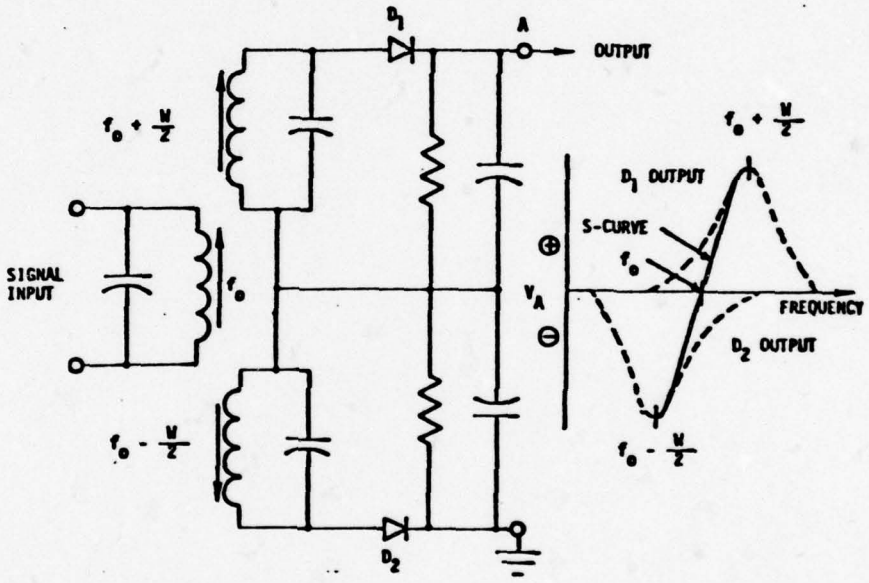

FIGURE 2 FM DISCRIMINATOR

frequency modulation due to the target is modeled as a zero-mean Gaussian random process; the non-zero mean case, including doppler effects, can be treated in a simple extension of the present results.

Previous efforts [1] have sought to calculate the detection performance of the FM correlator model (shown in Figure 1) by finding the probability distribution at the output of the multiplier. In the continuation of this approach, the exact distribution was found, and it is quite difficult to compute. An approximate method described also in [1], which used a common expression for the FM detector outputs valid under high carrier-to-noise power ratio (CNR) assumptions, also yields a rather complex probability density function (pdf) for the multiplier output. These latter results were, however, computable and some performance calculations were given in [1] which do not include the filter.

The previous performance (for no filter) was shown to be poor. The question remaining was whether "integration" or filtering of the multiplier output would improve the performance to an acceptable level.

B. Summary. In the present work, the output of the lowpass filter in Figure 1 is assumed to be Gaussian because of the integrating or summing effect of the filter. Therefore, the performance--receiver operating characteristics (ROC)--can be calculated using only the mean and variance of the filtered multiplier output as functions of the various bandwidths and CNR's involved. Analytical expressions are developed in Section III, based on the models and assumptions presented in Section II.

Using this approach, numerical results were computed and are displayed graphically in Section IV. Although further study is desirable in connection with direct system applications, the performances calculated so far indicate that the integrating filter does indeed improve the performance of the FM

correlator to an acceptable level, even for zero-mean Gaussian modulation. More detailed discussions of the effect of the various system parameters on the probability of detection accompany the figures in Section IV.

Recommendations for future work are given in Section V.

Acknowledgement: the authors wish to thank R. H. French for the development of the computer programs used to achive the numerical results, with the assistance of Y. K. Hong.

II. Models

A. Channel inputs. The inputs to the limiter/discriminators in the two channels are assumed to be of the form (A_i constant)

$$s_i(t) + n_i(t) = A_i \sin\left[\omega_o t + \phi_{mi}(t)\right] + n_{ci}(t)\cos\omega_o t + n_{si}(t)\sin\omega_o t$$

$$= R_i(t)\sin[\omega_o t + \phi_{mi}(t) + \psi_i(t)] \quad ; \quad i=1,2, \tag{1}$$

in which the narrowband noise components n_{ci}, n_{si} are assumed to be independent zero-mean Gaussian random variables from random processes with the correlation functions

$$E\left\{n_{ci}(t)n_{ci}(t+\tau)\right\} = E\left\{n_{si}(t)n_{si}(t+\tau)\right\} \tag{2}$$

$$= \sigma_{oi}^2 \rho_i(\tau).$$

In this work the noise spectra are assumed to be of Gaussian shape, that is,

$$S_i(f) = \frac{2\sigma_{oi}^2}{W_i\sqrt{\pi}} \exp\left\{-(f/W_i)^2\right\}, \quad f>0. \tag{3}$$

The noise bandwidth W_i here defined corresponds to a 4.34 dB roll-off of the spectrum. Correspondingly, we have

$$\rho_i(\tau) = \int_0^\infty df\, S_i(f)\cos 2\pi f\tau$$

$$= \exp\left\{-(\pi W_i \tau)^2\right\}. \tag{4}$$

The angle function $\phi_{mi}(t)$ indicated in (1) is assumed to be given by

$$\phi_{mi}(t) = \int^t d\xi\, m_i(\xi), \tag{5}$$

where the modulation $m_i(t)$ is assumed to be from a zero-mean Gaussian process with the correlation function

$$E\left\{m_i(t)m_i(t+\tau)\right\} = P_m\rho_m(\tau) = P_m\exp\left\{-(\pi W_m\tau)^2\right\}. \tag{6}$$

where W_m is defined as the 4.34 dB bandwidth of the modulating process. Further, it is assumed that

$$\begin{aligned} m_1(t) &\equiv m(t) \\ m_2(t) &\equiv m(t-\Delta t), \end{aligned} \tag{7}$$

so that in (6) no channel subscript (i) is required.

In (1) also we have

$$\left.\begin{aligned} R_i^2(t) &= [A_i + n_{1i}(t)]^2 + [n_{2i}(t)]^2 \\ \psi_i(t) &= \tan^{-1}\left[\frac{n_{2i}(t)}{A_i+n_{1i}(t)}\right] \end{aligned}\right\} \tag{8}$$

where

$$\begin{aligned} n_{1i}(t) &\triangleq n_{ci}(t)\sin\phi_{mi}(t) + n_{si}(t)\cos\phi_{mi}(t) \\ n_{2i}(t) &\triangleq n_{ci}(t)\cos\phi_{mi}(t) - n_{si}(t)\sin\phi_{mi}(t). \end{aligned} \tag{9}$$

The transformed processes $n_{1i}(t)$, $n_{2i}(t)$ are also independent, zero-mean Gaussian.

B. Channel outputs. The limiter/discriminator operations diagrammed in Figure 3 are assumed to be ideal so that their outputs are

$$z_i(t) = m_i(t) + \dot{\psi}_i(t), \tag{10}$$

neglecting any constant factors. It should be noted that $\dot{\psi}$ and m are not independent.

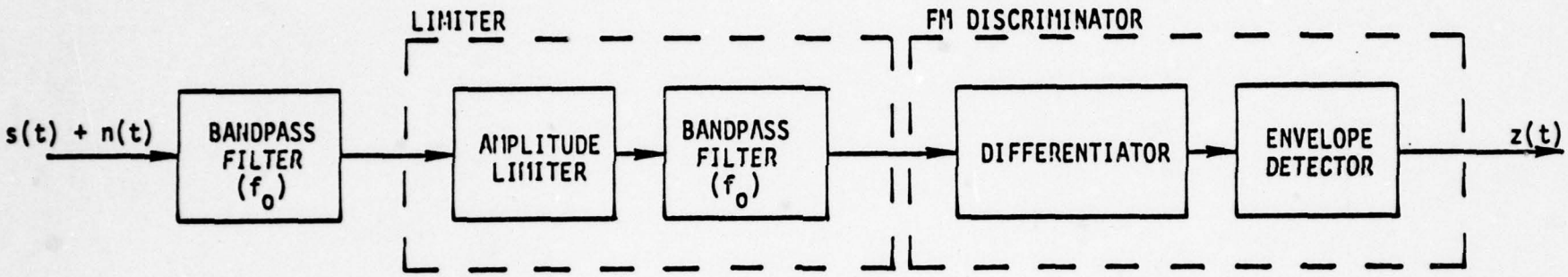

FIGURE 3 FM DETECTOR MODEL

This fact is understood from

$$\dot{\psi}_i(t) = \frac{(A_i+n_{1i})\dot{n}_{2i}-\dot{n}_{1i}n_{2i}}{(A_i+n_{1i})^2+(n_{2i})^2} \tag{11}$$

and from (9), in which it is evident that the derivatives of the noise terms contain $\dot{\phi}_{mi} \equiv m_i$. Thus we can also write

$$z_i(t) = m_i(t)\left[\frac{A_i(A_i+n_{1i})}{(A_i+n_{1i})^2+n_{2i}^2}\right] + \frac{(A_i+n_{1i})n_{4i}-n_{3i}n_{2i}}{(A_i+n_{1i})^2+n_{2i}^2} \tag{12}$$

using

$$\begin{aligned} n_{3i} &= \dot{n}_{ci}\sin\phi_{mi} + \dot{n}_{si}\cos\phi_{mi} \\ n_{4i} &= \dot{n}_{ci}\cos\phi_{mi} - \dot{n}_{si}\sin\phi_{mi}. \end{aligned} \tag{13}$$

Under this representation, n_{1i}, n_{2i}, n_{3i}, n_{4i} are independent.

The probability density functions for z_1 and z_2 are derived in the appendix, with m_1 and m_2 as parameters, in order to calculate their means.

C. Filters and Correlator Outputs.

Using h(t) for the filter impulse response, the correlator output is given by

$$z(t) = \int_{-\infty}^{\infty} d\tau\, h(\tau)z_1(t-\tau)z_2(t-\tau). \tag{14}$$

It is assumed that every T seconds the filter output is sampled (to be compared to a threshold) and the filter is reset. Thus the samples are written

$$z(T) = \int_{0}^{T} d\tau\, h(\tau)z_1(T-\tau)z_2(T-\tau). \tag{15}$$

In this work three types of filters are to be considered:

$$\text{Filter 1: } h_1(t) = \begin{cases} \frac{1}{T}, & 0<t<T \\ 0, & \text{otherwise} \end{cases} \qquad \text{(Integrate and dump)} \qquad (16)$$

$$\text{Filter 2: } h_2(t) = \begin{cases} \frac{1}{RC} e^{-t/RC}, & t>0 \\ 0, & t<0 \end{cases} \qquad \text{(Singled-tuned LPF)} \qquad (17)$$

$$\text{Filter 3: } h_3(t) = \begin{cases} \omega_b \sqrt{2}\, e^{-\omega_b t/\sqrt{2}} \sin(\omega_b t/\sqrt{2}), & t>0 \\ 0, & t<0 \end{cases} \qquad (18)$$

(2-pole Butterworth LPF)

The 3-dB bandwidths of filters 2 and 3 are

$$B_2 = \frac{1}{2\pi RC}$$

and

$$B_3 = \omega_b/2\pi. \qquad (19)$$

D. Detection. The Neyman-Pearson model of detection will be used. Under the null hypothesis,

$$z(T|H_0) \sim N(\mu_0, \sigma_{z0}^2)$$

with

$$H_0: \text{CNR}_1 = \text{CNR}_2 = 0.$$

The alternative hypothesis is

$$H_1: \text{CNR}_1, \text{CNR}_2 \neq 0$$

for which it is assumed $z(T|H_1) \sim N[\mu(T), \sigma_z^2(T)]$

Probability of false alarm is therefore given by

$$P_{F_A} = \int_{\eta}^{\infty} dz\, p(z|H_0) = \frac{1}{2} - \frac{1}{2}\text{erf}\left[\frac{\eta-\mu_0}{\sigma_{z0}\sqrt{2}}\right] \tag{20}$$

For a given value of P_{F_A}, then, we can compute the threshold η. The probability of detection becomes

$$P_D = \int_{\eta}^{\infty} dz\, p(z|H_1) = \frac{1}{2} - \frac{1}{2}\text{erf}\left[\frac{\eta-\mu(T)}{\sigma_z(T)\sqrt{2}}\right] \tag{21}$$

where P_D is a function of the CNR's.

III. Analytical Results.

A. Mean of Correlator Output. From (13) we have

$$\begin{aligned} E\{z(T)\} &\equiv \mu(T) \\ &= \int_0^T d\tau\, h(\tau) E\{z_1(T-\tau)z_2(T-\tau)\}. \end{aligned} \tag{22}$$

Now, the expectation is taken over both modulation and noise; and for stationary processes,

$$\begin{aligned} E\{z_1(T-\tau)z_2(T-\tau)\} &= E\{z_1(t)z_2(t)\} \\ &= E_m\{E_{n|m}\{z_1(t)z_2(t)\}\} \\ &= E_m\{E_{n_1|m_1}\{z_1(t)\}E_{n_2|m_2}\{z_2(t)\}\}. \end{aligned} \tag{23}$$

From the appendix

$$E_{n_i|m_i}\{z_i(t)\} = m_i(t)[1-e^{-h_i^2}] \tag{24}$$

where

$$h_i^2 \equiv \text{CNR}_i = A_i^2/2\sigma_{oi}^2. \tag{25}$$

Therefore,

$$\mu(T) = E\{m_1(t)m_2(t)\}(1-e^{-h_1^2})(1-e^{-h_2^2}) \int_0^T d\tau\, h(\tau)$$

$$= P_m\rho_m(\Delta t)(1-e^{-h_1^2})(1-e^{-h_2^2}) \int_0^T d\tau\, h(\tau) \tag{26}$$

using the notation of (6).

B. Variance of Correlator. First, the mean square is written

$$E\{z^2(T)\} = \int_0^T d\nu \int_0^T d\tau\, h(\nu)h(\tau)E\{z_1(T-\nu)z_2(T-\nu)z_1(T-\tau)z_2(T-\tau)\}$$

$$= \int_0^T d\nu \int_0^T d\tau\, h(\nu)h(\tau)R_x(\tau-\nu), \tag{27}$$

where $R_x(\tau)$ is the correlation function of the multiplier output. In the appendix it is shown that (27) can also be written

$$E\{z^2(T)\} = 2\int_0^T d\tau\, R_x(\tau)g(\tau) \tag{28}$$

with $g(\tau)$ the filter autocorrelation function:

$$g(\tau) \equiv \int_0^{T-\tau} d\nu\, h(\nu)h(\nu+\tau). \tag{29}$$

The square of the mean (26) is

$$\mu^2(T) = P_m^2\rho_m^2(\Delta t)\left(1-e^{-h_1^2}\right)^2\left(1-e^{-h_2^2}\right)^2 \int_0^T d\nu \int_0^T d\tau\, h(\nu)h(\tau)$$

$$= P_m^2\rho_m^2(\Delta t)\left(1-e^{-h_1^2}\right)^2\left(1-e^{-h_2^2}\right)^2 2\int_0^T d\tau\, g(\tau). \tag{30}$$

In this expression the double integral was reduced in the same way as it was in the transition from equations (27) to (28). Thus the variance is

$$\sigma_z^2(T) = E\{z^2(T)\} - \mu^2(T)$$

$$= 2\int_0^T d\tau\, g(\tau)\{R_x(\tau) - P_m^2\rho_m^2(\Delta t)(1-e^{-h_1^2})^2(1-e^{-h_2^2})^2\}. \qquad (31)$$

Now $R_x(\tau)$ is found to be

$$R_x(\tau) = E\{z_1(t)z_2(t)z_1(t+\tau)z_2(t+\tau)\}$$

$$= E_m\{E_{n_1|m}\{z_1(t)z_1(t+\tau)\}E_{n_2|m}\{z_2(t)z_2(t+\tau)\}\}$$

$$= E_m\{R_{z_1|m_1}(\tau)R_{z_2|m_2}(\tau)\}, \qquad (32)$$

where the $R_{z_i|m_i}(\tau)$ are the (conditional) correlation functions of the FM detector outputs. The correlation function of an FM detector is known to be of the form [2, chapter 13]

$$R_{z_i|m_i}(\tau) = m_i(t)m_i(t+\tau)(1-e^{-h_i^2})^2 + f_i(\tau) \qquad (33)$$

where

$$f_i(\tau) \equiv f[\rho_i(\tau), \dot{\rho}_i(\tau), \ddot{\rho}_i(\tau); h_i^2] \qquad (34)$$

and

$$f = \frac{\dot{\rho}^2}{2\rho^2}\left\{1 - \frac{2e^{-h^2}}{1-\rho} + \frac{1+\rho}{1-\rho}e^{-2h^2/(1+\rho)}\right.$$

$$\left. -e^{-h^2/\rho}\left(\frac{\ddot{\rho}\rho}{\dot{\rho}^2} + \frac{h^2}{\rho} - 1\right)\left[Ei\left(\frac{h^2}{\rho}\right) - 2Ei\left(\frac{1-\rho}{\rho}h^2\right) + Ei\left(\frac{1-\rho}{1+\rho}\frac{h^2}{\rho}\right)\right]\right\} \qquad (35)$$

in which the Ei(x) represents the exponential integral

$$Ei(x) \triangleq \int_{-\infty}^{x} dt\, \frac{e^t}{t}\,, \quad x>0, \tag{36}$$

and the $\rho_i(\tau)$ are noise correlation functions (cf (2)-(4)).

In consideration of (33)-(36), $R_x(\tau)$ becomes

$$\begin{aligned} R_x(\tau) = {} & \left(1-e^{-h_1^2}\right)^2\left(1-e^{-h_2^2}\right)^2 E\left\{m_1(t)m_1(t+\tau)m_2(t)m_2(t+\tau)\right\} \\ & + P_m\rho_m(\tau)\left[(1-e^{-h_2^2})^2 f_2(\tau) + (1-e^{-h_2^2})^2 f_1(\tau)\right] \\ & + f_1(\tau)f_2(\tau). \end{aligned} \tag{37}$$

Since m(t) is Gaussian,

$$\begin{aligned} & E\left\{m_1(t)m_1(t+\tau)m_2(t)m_2(t+\tau)\right\} \\ & \quad = E\left\{m(t)m(t+\tau)m(t-\Delta t)m(t+\tau-\Delta t)\right\} \\ & \quad = P_m^2\left[\rho_m^2(\tau) + \rho_m^2(\Delta t) + \rho_m(\tau-\Delta t)\rho_m(\tau+\Delta t)\right]. \end{aligned} \tag{38}$$

Substituting (38) in (37) and (31) gives

$$\begin{aligned} \sigma_z^2(T) = 2\int_0^T d\tau\, g(\tau)\Big\{ & P_m^2(1-e^{-h_1^2})^2(1-e^{-h_2^2})^2\left[\rho_m^2(\tau) + \rho_m(\tau-\Delta t)\rho_m(\tau+\Delta t)\right] \\ & + P_m\rho_m(\tau)\left[(1-e^{-h_1^2})^2 f_2(\tau) + (1-e^{h_2^2})f_1(\tau)\right] + f_1(\tau)f_2(\tau)\Big\}. \end{aligned} \tag{39}$$

IV. Numerical Results

After the necessary analytical expressions for the mean and variance of the filter output were developed, detection probabilities were calculated via numerical integration, according to the model of detection shown in Section II-D.

In setting up the calculations, the following basic parameters were identified:

h^2	carrier SNR (CNR)
$\gamma = P_m/(2\pi W)^2$	ratio of mean square frequency modulation to square of channel bandwidth
WT	channel bandwidth-time product
$\varepsilon = W_m/W$	ratio of modulation bandwidth to channel bandwidth
BT	filter bandwidth-time product

In all of the computed cases, the modulations in the channels were assumed to be aligned in time ($\Delta t = 0$). The reference case for the calculations to be shown was chosen to be

$$\gamma = 1,\ WT = 5,\ BT = .3,\ \varepsilon = 1. \qquad (40)$$

A. Receiver operating characteristics.

The probability of detection (P_D) at the filter output, as a function of CNR, is displayed in Figures 4 - 7 for probabilities of false alarm equal to 10^{-2}, 10^{-3}, and 10^{-4}. Because of the rather steep slope with the linear P_D scale of Figure 4, the expanded, probability scale of Figures 5 - 7 is to be preferred for discussion. Several interesting features of the figures invite comment.

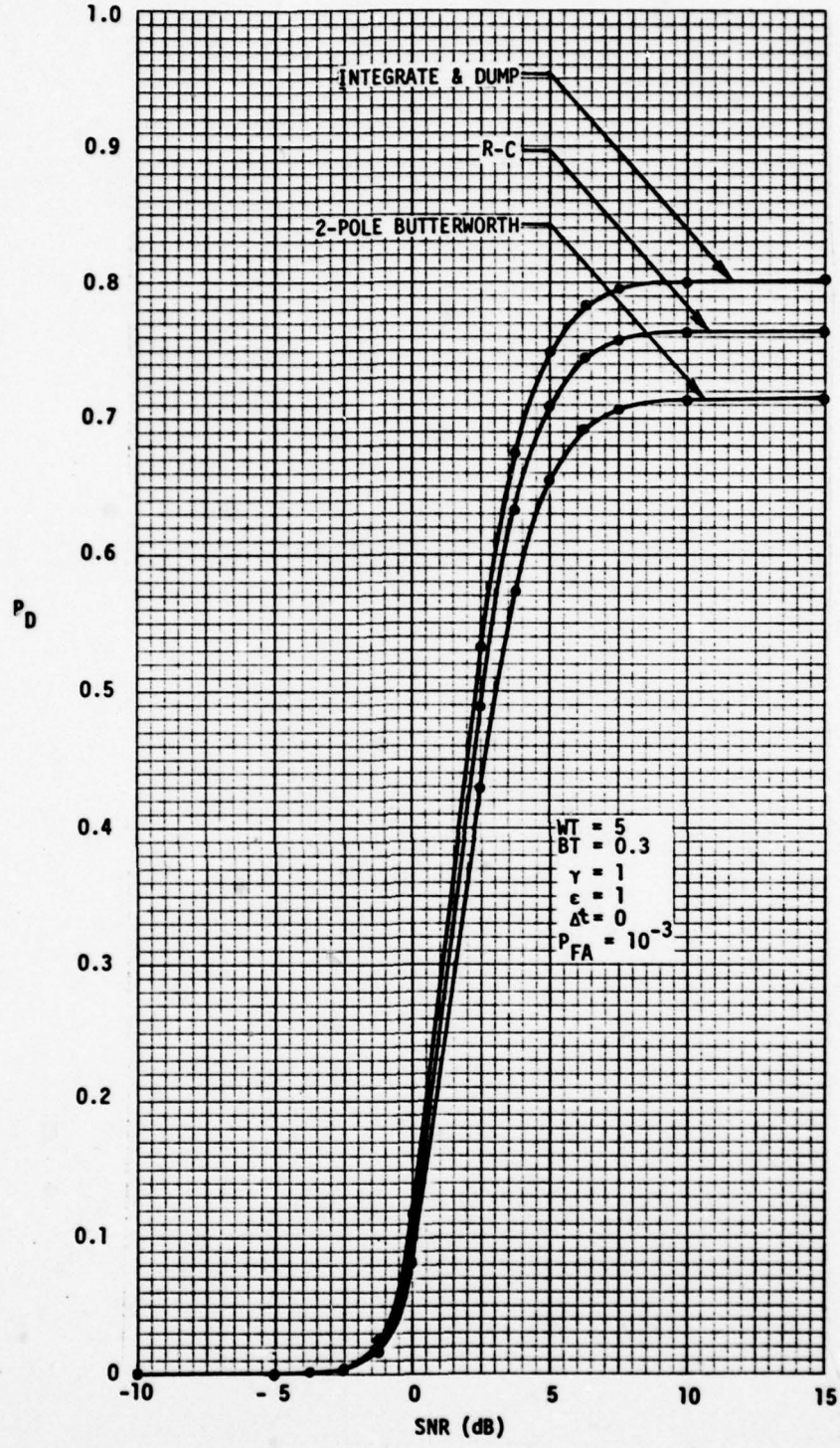

FIGURE 4 FM CORRELATOR RECEIVER OPERATING CHARACTERISTICS (LINEAR SCALE)

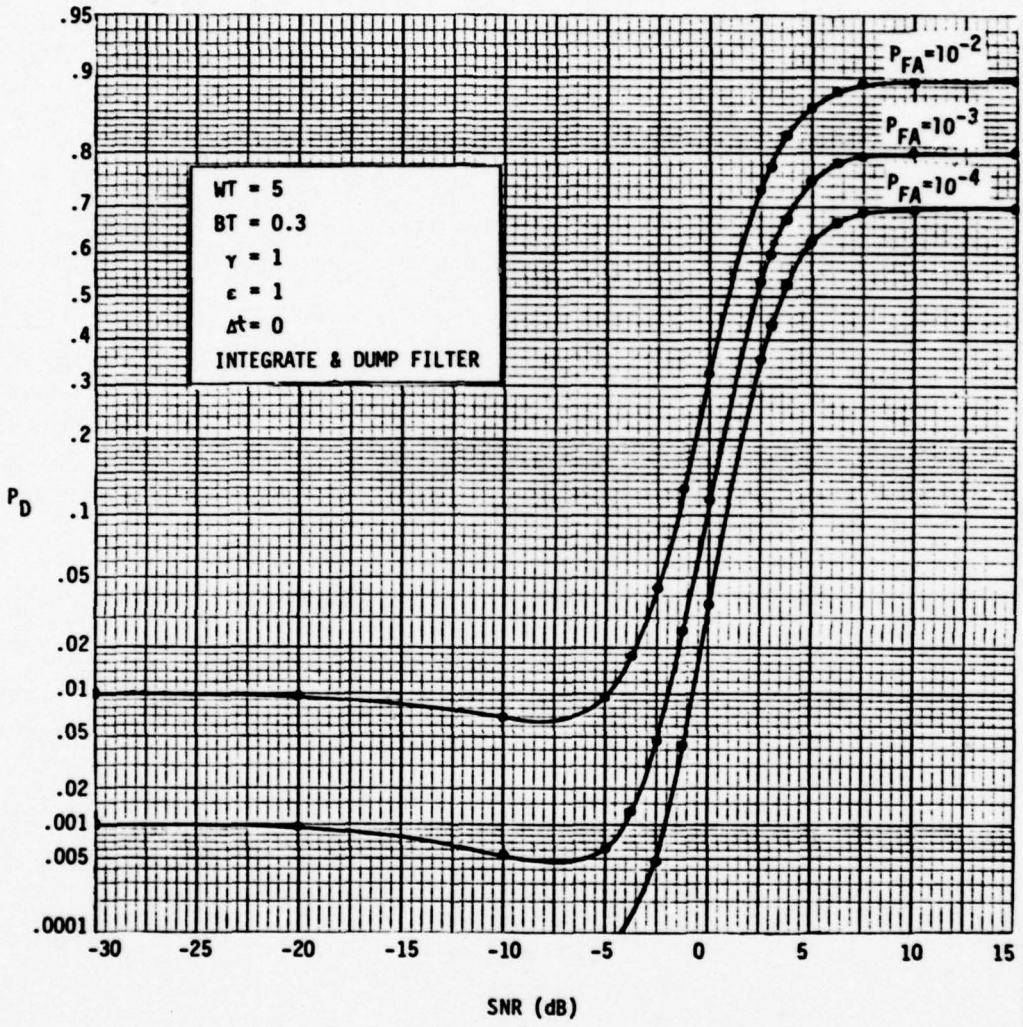

FIGURE 5 FM CORRELATOR RECEIVER OPERATING CHARACTERISTICS (INTEGRATE-AND-DUMP FILTER)

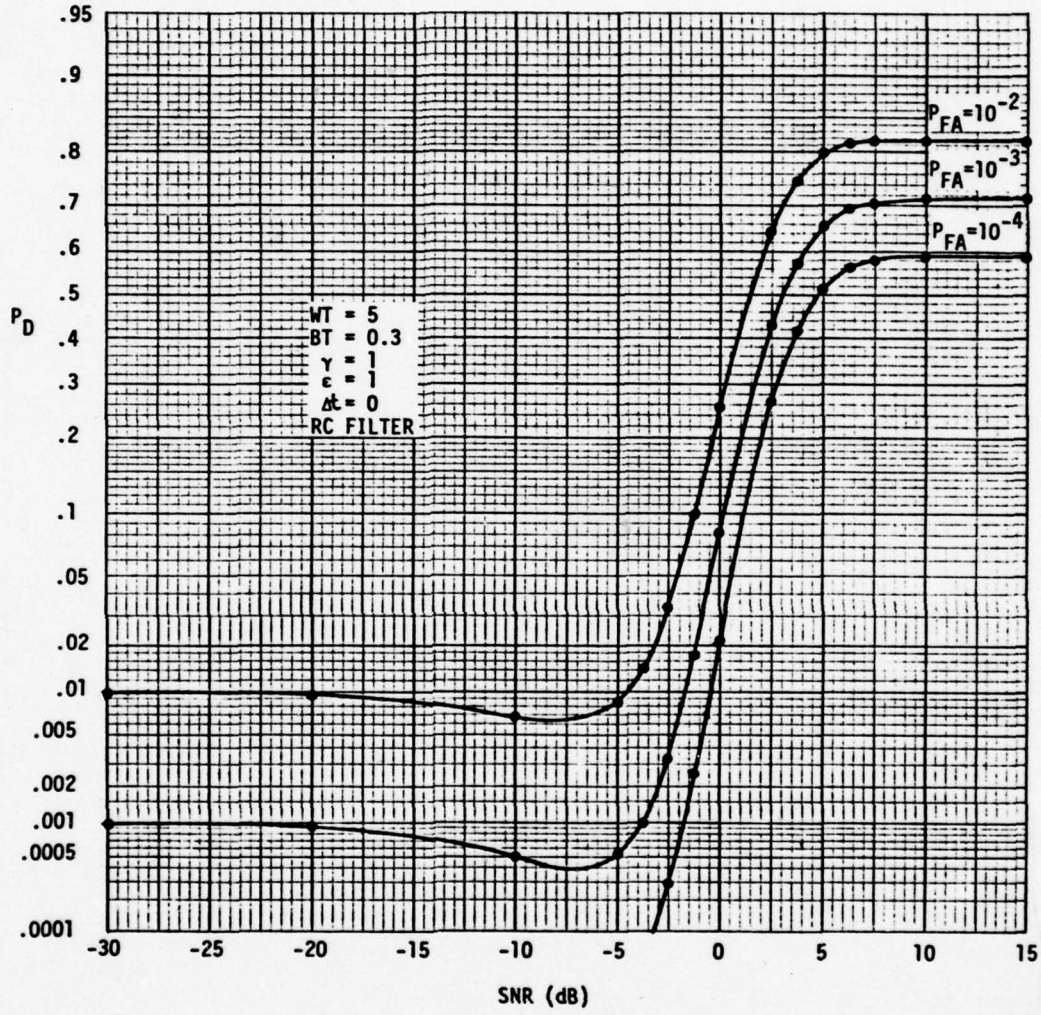

FIGURE 6 FM CORRELATOR RECEIVER OPERATING CHARACTERISTICS (RC FILTER)

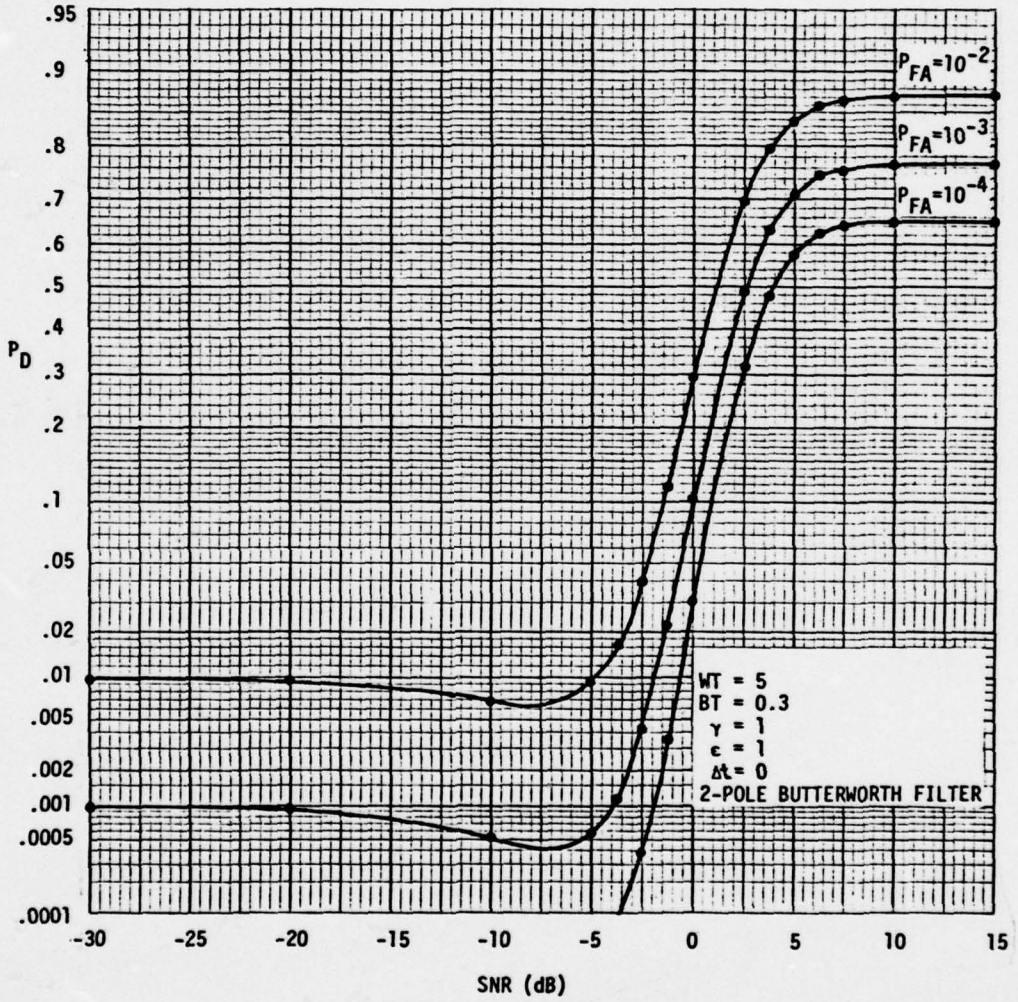

FIGURE 7 FM CORRELATOR RECEIVER OPERATING CHARACTERISTICS (2-POLE BUTTERWORTH FILTER)

Limiting values. The value of P_D for very small CNR, of course, has an immediate interpretation:

$$P_D \to P_{FA} \text{ as } CNR \to 0 \qquad (41)$$

However, the fact that P_D approaches a value less than one for large SNR is, at first sight, somewhat unusual because we are accustomed to thinking of SNR as a location parameter for the pdf of the decision variable. In this FM situation, though, the SNR involved is actually the CNR, and what is "happening" in Figures 4 - 7 can be described very simply. At high CNR the correlator output approaches that of the noiseless case, in which (see (26) and (39))

$$\mu(T) = C_1 E\{m^2\} \qquad (42)$$

$$= C_1 P_m$$

and

$$\sigma_z^2(T) = C_2 P_m^2 \qquad (43)$$

Thus for Gaussian frequency modulation, both the mean and standard deviation of the correlator output are directly proportional to the mean square of the modulation. For all values of P_m, there is always a portion of the distribution which falls below the threshold; thus $P_D < 1$ as $CNR \to \infty$.

Transition values. For CNR neither very large nor very small, we may think of the correlator output pdf as the outcome of a "battle" between the noise only case and the noiseless case:

	noise only	transition	noiseless
mean	$\mu_n = 0$	μ_{n+m}	μ_m
variance	σ_n^2	σ_{n+m}^2	σ_m^2.

As so often occurs in nonlinear systems, one effect captures or suppresses the other; therefore the transition from a low P_D to a high value takes place over a relatively small interval of CNR values.

What is intriguing is that there is an interval over which $P_D < P_{FA}$. It seems that, as CNR increases from zero, for a while the net (noise + modulation) distribution begins to have a sharper peak (smaller σ) before the mean value begins to shift.

B. Parameter variations.

Some calculations were designed to explore the effect of departures of the various parameters from the reference case (40) for CNR = 10 dB.

In Figure 8, γ is varied. As anticipated in the previous discussion, increasing γ (increasing P_m) causes the limiting value of P_D to increase, but this effect saturates due to the fact that both mean and variance depend upon P_m. Therefore, increasing "modulation power" beyond a certain point is not productive.

WT is varied in Figure 9, indicating that, for W fixed, increasing T improves detection performance by integrating longer the (nonzero) multiplier mean when there is modulation. For fixed T, the interpretation is less clear, since postulating a variation in W and holding γ constant involves increasing P_m also.

In Figure 10, ε, the ratio W_m/W, is decreased from its reference value of unity. The effect is to decrease the value of P_D (i.e., $P_D \propto \varepsilon$). If a modulation index be defined as

$$\beta \triangleq \frac{\sqrt{P_m}}{2\pi W_m} = \sqrt{\gamma/\varepsilon} \qquad (44)$$

the bandwidth of the modulated carrier may be approximated by

$$B.W. \simeq 2W_m(1 + \beta) = 2W(\varepsilon + \sqrt{\gamma}) \qquad (45)$$

For fixed γ, then, bandwidth of the modulated carrier is proportional to ε, and the effect shown in Figure 10 can be attributed to variation in correlator output SNR, as demonstrated in [6].

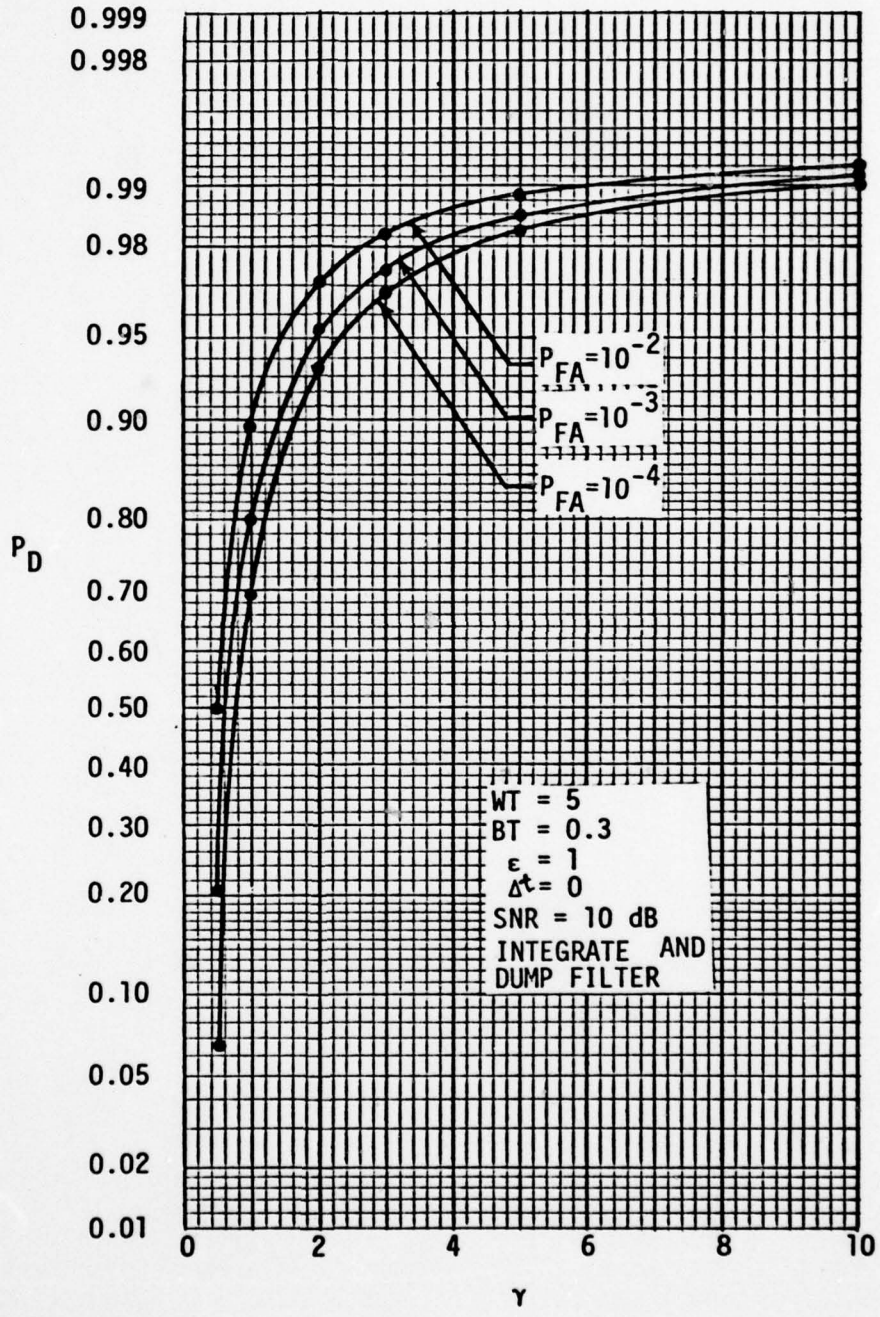

FIGURE 8 EFFECT OF MODULATION POWER ON PROBABILITY OF DETECTION

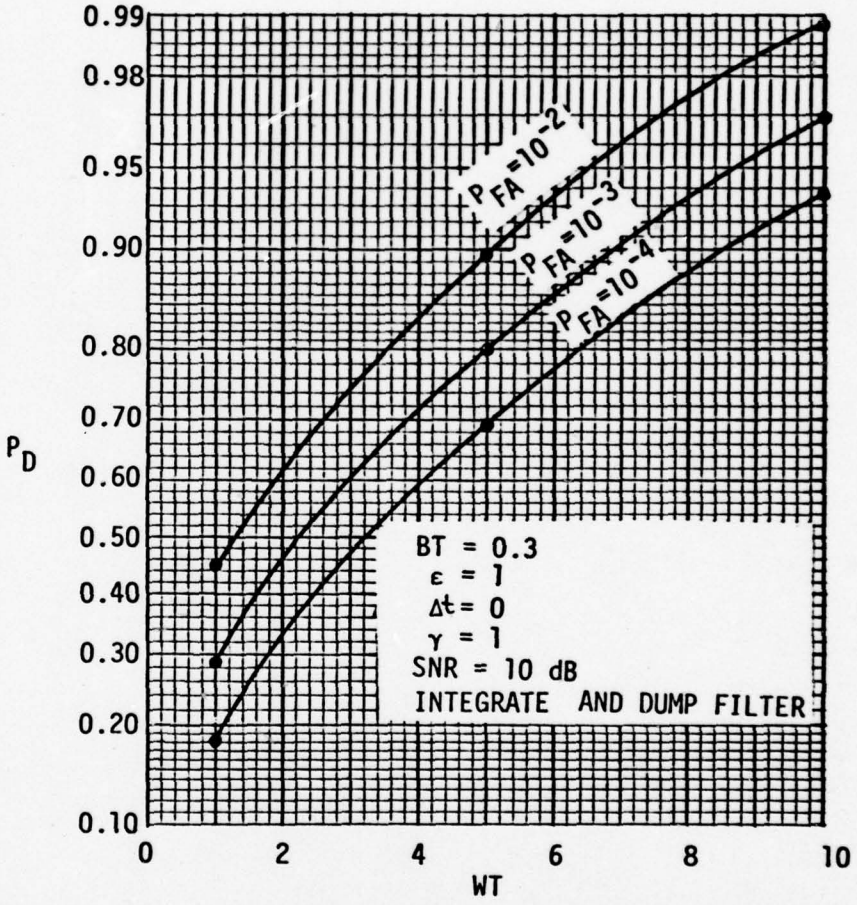

FIGURE 9 EFFECT OF BANDWIDTH-TIME PRODUCT ON PROBABILITY OF DETECTION

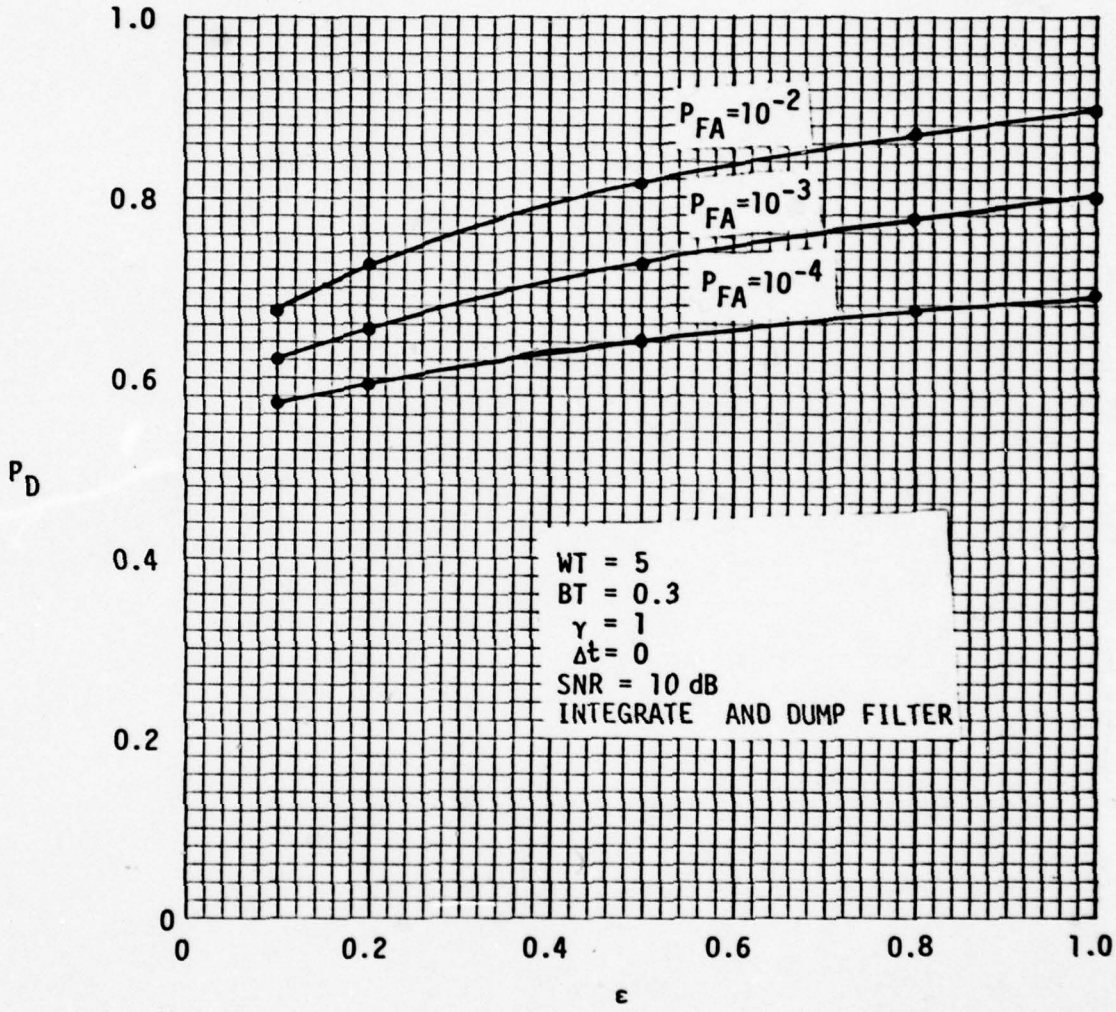

FIGURE 10 EFFECT OF MODULATION BANDWIDTH ON PROBABILITY OF DETECTION

A most interesting effect is seen in Figure 11 , in which the filter bandwidth-time product (BT) is varied for the case of the 2-pole Butterworth filter. Evidently there is an optimum value of BT in the neighborhood of BT = .4. A similar phenomenon was reported in [7] and attributed to a tradeoff between noise rejection and signal rejection; as the filter bandwidth decreases, at first more noise is rejected than signal, causing improved output SNR and P_D. Reduction of filter bandwidth beyond a certain point, however, rejects more signal than noise. Thus there is an optimum value of BT which in some sense matches the signal (in this case, the modulation), and which will depend upon CNR.

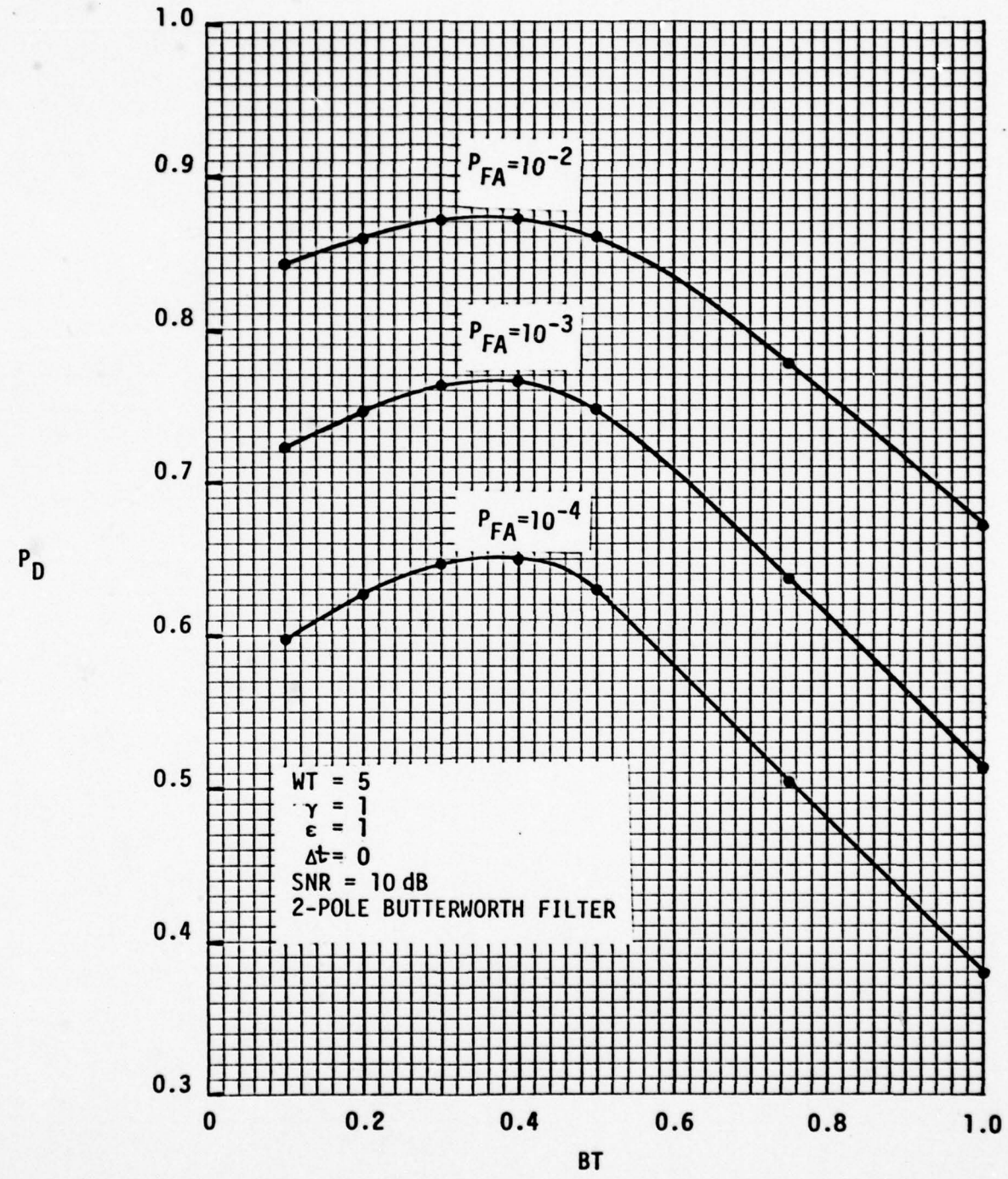

FIGURE 11 EFFECT OF FILTER BANDWIDTH ON PROBABILITY OF DETECTION (2-POLE BUTTERWORTH FILTER)

V. Concluding Discussion.

The question which has motivated this work - whether an FM correlator (with integrating filter) can perform acceptably as a detector - has been answered in the affirmative. For, as demonstrated numerically in the figures of the previous section, probabilities of detection close to unity can be achieved for arbitrary false alarm rates by manipulation of receiver parameters. Having answered this basic question (with much effort initially), only a sampling of parametric investigations have been carried out so far. For example, with the computer programs now in use, it is a straightforward effort to determine the minimum detectable signal, both in terms of CNR and modulation power (P_m), required to assure a given P_D for fixed P_{FA}. Several studies of this type, characterizing the basic performance tradeoffs associated with FM correlation detectors, would be quite interesting and, if widely disseminated, would provide system designers with fuel for thought.

One basic study which seems to have a significant potential for system application is the case of random modulation (treated herein) but with nonzero, time-varying mean. This model corresponds to narrowband emissions of uncertain or varying center frequency, and subject to doppler shifts.

Further investigations should begin to focus on system applications, taking into account specifically doppler (motion) models and details of frequency conversion circuitry, in order to assess accurately potential system performance. The future study should address itself to the problem of detecting multiple narrowband spectra as an extension of the current effort. Also, labaratory simulation should be considered in future efforts.

APPENDICES

A. pdf for the Output of the FM Limiter-Discriminator

In this derivation a slightly different form for the FM channel outputs z_i is used. Instead of (10), let us write

$$z_i(t) = \dot{\theta}_i(t) \tag{A-1}$$

where the channel input is written

$$A_i\sin[\omega_o t + \phi_{si}(t)] + n_{ci}(t)\cos\omega_o t + n_{si}(t)\sin\omega_o t$$

$$= R_i(t)\sin[\omega_o t + \theta_i(t)]. \tag{A-2}$$

Since, under this representation,

$$\theta_i(t) = \tan^{-1}\left\{\frac{n_{ci} + A_i\sin\theta_i(t)}{n_{si} + A_i\cos\theta_i(t)}\right\}, \tag{A-3}$$

we have

$$\dot{\theta}_i(t) = z(t) = \frac{u\dot{v} - v\dot{u}}{u^2 + v^2} \tag{A-4}$$

using $u = n_{si} + A_i\cos\phi_{mi}$ and $v = n_{ci} + A_i\sin\phi_{mi}$. (A-5)

Input Distribution

At the same instant, $(n_{ci}, n_{si}, \dot{n}_{ci}, \dot{n}_{si})$ are mutually independent Gaussian variates [3] with zero means and

$$\begin{aligned} \text{var}(n_c) &= \text{var}(n_s) \triangleq \sigma_o^2 \\ \text{var}(\dot{n}_c) &= \text{var}(\dot{n}_s) \triangleq \sigma_1^2 \end{aligned} \tag{A-6}$$

where, for a flat noise spectrum over the passband b (in Hertz), [4],

$$\sigma_1^2 = \sigma_o^2/k = 4\pi^2\sigma_o^2 b^2/3. \tag{A-7}$$

Thus the variates $(u, v, \dot{u}, \dot{v})$ have the probability density function (pdf)

$$p_o(u,v,\dot{u},\dot{v}) = (2\pi\sigma_o\sigma_1)^{-2}\exp\left\{-\frac{(u-\bar{u})^2 + (v-\bar{v})^2}{2\sigma_o^2} - \frac{(\dot{u}-\bar{\dot{u}})^2 + (\dot{v}-\bar{\dot{v}})^2}{2\sigma_1^2}\right\},$$

$$-\infty<(u,v,\dot{u},\dot{v})<\infty. \qquad \text{(A-8)}$$

Mean values are taken to be

$$\begin{aligned}
\bar{u} &= A\cos\phi_{mi},\ \bar{v} = A\sin\phi_{mi} \\
\bar{\dot{u}} &= -mA\sin\phi_{mi} + \dot{A}\cos\phi_{mi} \qquad \text{(A-9)} \\
\bar{\dot{v}} &= mA\cos\phi_{mi} + \dot{A}\sin\phi_{mi}
\end{aligned}$$

Output Distribution

Consider the transformation of variables (dropping the subscript i)

$$\begin{aligned}
u &= R\cos\theta && 0\le R<\infty \\
v &= R\sin\theta && 0\le\theta\le 2\pi \\
\dot{u} &= \xi\cos\theta - \eta\sin\theta && -\infty<\xi<\infty \qquad \text{(A-10)} \\
\dot{v} &= \xi\sin\theta + \eta\cos\theta && -\infty<\eta<\infty
\end{aligned}$$

for which

$$z = \frac{u\dot{v} - v\dot{u}}{u^2 + v^2} = \eta/R. \qquad \text{(A-11)}$$

The variable ξ can be interpreted as $\dot{R}$, the derivative of the envelope, and η, as $R\dot{\theta}$, θ being the phase of the input waveform as given by (A-2).

The Jacobian of the transformation is R, so that the pdf of the new variables is

$$p_1(R,\theta,\xi,\eta) = R\,p_0(R\cos\theta,\ R\sin\theta,\ \xi\cos\theta - \eta\sin\theta,\ \xi\sin\theta + \eta\cos\theta)$$

$$= R(2\pi\sigma_0\sigma_1)^{-2}\exp\left\{-\frac{1}{2\sigma_0^2}\left[R^2 + A^2 - 2RA\cos(\theta-\phi_m)\right]\right.$$

$$-\frac{1}{2\sigma_1^2}\left[\xi^2 + \eta^2 + m^2A^2 + \dot{A}^2 - 2(mA\xi-\eta\dot{A})\sin(\theta-\phi_m)\right.$$

$$\left.\left.-2(\xi\dot{A}+\eta mA)\cos(\theta-\phi_m)\right]\right\}. \quad \text{(A-12)}$$

Eliminating ξ by integration, we have

$$p_2(R,\theta,\eta) = \int_{-\infty}^{\infty} d\xi\ p_1(R,\theta,\xi,\eta)$$

$$= R\left[(2\pi)^{3/2}\sigma_0^2\sigma_1\right]^{-1}\exp\left\{-\frac{R^2 + A^2}{2\sigma_0^2} - \frac{\eta^2}{2\sigma_1^2}\right\} \quad \text{(A-13)}$$

$$\times\ \exp\left\{\frac{RA}{\sigma_0^2}\cos(\theta-\phi_m) - \frac{1}{2\sigma_1^2}\left[a^2\cos^2(\theta-\phi_m+\phi_a) - 2\eta a\cos(\theta-\phi_m-\phi_a)\right]\right\}$$

using $\quad a^2 = m^2A^2 + \dot{A}^2, \quad \phi_a = \tan^{-1}(\dot{A}/mA). \quad \text{(A-14)}$

The terms in the second exponential may be written also

$$Rb\cos(\theta-\phi_m+\phi_a-\phi_b) - \frac{a^2}{4\sigma_1^2} - \frac{a^2}{4\sigma_1^2}\cos 2(\theta-\phi_m+\phi_a) \quad \text{(A-15)}$$

with
$$\left.\begin{aligned} R^2b^2 &= \left(\frac{\eta a}{\sigma_1^2}\cos\phi_a + \frac{RA}{\sigma_0^2}\right)^2 + \left(\frac{\eta a}{\sigma_1^2}\sin\phi_a\right)^2 \\ \text{and}\quad \phi_b &= \tan^{-1}\left[\left(\frac{\eta a}{\sigma_1^2}\sin\phi_a\right)\Big/\left(\frac{\eta a}{\sigma_1^2}\cos\phi_a + \frac{RA}{\sigma_0^2}\right)\right]. \end{aligned}\right\} \quad \text{(A-16)}$$

Defining a second transformation of variables (with Jacobian = w)

$$\eta = zw \quad , \quad 0 \leq w < \infty$$
$$R = w \quad , \quad -\infty < z < \infty \tag{A-17}$$

results in the new joint pdf

$$p_3(w,\theta,z) = \left[(2\pi)^{3/2}\sigma_o^2\sigma_1\right]^{-1} w^2 e^{-h^2} \exp\left\{-\frac{w^2}{2\sigma_o^2}(1 + kz^2)\right\}$$
$$x \exp\left\{w\, b \cos(\theta - \phi_m + \phi_a - \phi_b) - \frac{a^2}{2\sigma_1^2}\cos^2(\theta - \phi_m + \phi_a)\right\} \tag{A-18}$$

The integration of (A-18) with respect to the variable w involves an integral of the form[1]

$$\int_0^\infty dw\, w^2 e^{-\gamma w^2 + 2\sqrt{\gamma u}\, w \cos\beta}$$
$$= \frac{\sqrt{\pi}}{2}\gamma^{-3/2}\left\{\sqrt{\frac{u}{\pi}}\cos\beta + (u\cos^2\beta + \tfrac{1}{2})e^{u\cos^2\beta}\left[1 + \operatorname{erf}(\sqrt{u}\cos\beta)\right]\right\} \tag{A-19}$$
$$= \frac{\sqrt{\pi}}{2}\gamma^{-3/2}\left\{\sqrt{\frac{u}{\pi}}\cos\beta + (u\cos^2\beta + \tfrac{1}{2})e^{u\cos^2\beta}\right.$$
$$\left. x \left[1 + \sqrt{\frac{u}{\pi}}\cos\beta\, {}_1F_1\left(\tfrac{1}{2}; 3/2; u\cos^2\beta\right)\right]\right\} \tag{A-20}$$

where

$$\left.\begin{aligned} \gamma &\equiv \frac{1+kz^2}{2\sigma_o^2} \\ \beta &\equiv \theta - \phi_m + \phi_a - \phi_b \end{aligned}\right\} \tag{A-21}$$

---

1. Using [5], #'s 3.462.7, 9.236.1

and

$$(1+kz^2)\,u \equiv \frac{b^2}{4\gamma} = h^2 + \left(\frac{a^2}{2\sigma_o^2}\right)k^2z^2 + 2(kz)\left(\frac{a}{\sigma_o\sqrt{2}}\right)h\cos\phi_a; \tag{A-22}$$

${}_1F_1$ denotes the confluent hypergeometric function, and $h^2 \equiv A^2/2\sigma_o^2$.

Note that for $\dot{A} = 0$, $a = mA$ and $\phi_b = 0$; also,

$$u(z)\Big|_{\dot{A}=0} = \frac{(1+mkz)^2}{1+kz^2}\,h^2. \tag{A-23}$$

Using (15), we have

$$p_4(\theta,z) = \frac{\sqrt{k}}{2\pi(1+kz^2)^{3/2}}\,e^{-h^2}\exp\left\{-\frac{a^2}{2\sigma_1^2}\cos^2(\beta+\phi_b)\right\}$$

$$\times\left\{\sqrt{\frac{u(z)}{\pi}}\cos\beta + \left[u(z)\cos^2\beta + \tfrac{1}{2}\right]e^{u(z)\cos^2\beta}\right. \tag{A-24}$$

$$\left. + \left[u(z)\cos^2\beta + \tfrac{1}{2}\right]e^{u(z)\cos^2\beta}\,{}_1F_1\left[\tfrac{1}{2};3/2;u(z)\cos^2\beta\right]\right\}.$$

Only the second term of (A-24) survives integration with respect to θ, leaving

$$p_5(z) = \frac{\sqrt{k}}{(1+kz^2)^{3/2}}\exp\left\{-h^2 - \frac{a^2}{4\sigma_1^2} + \frac{u(z)}{2}\right\}\sum_{n=0}^{\infty}\varepsilon_n I_n\left[\rho(z)\right]$$

$$\times\frac{1}{2\pi}\int_0^{2\pi}d\theta\left\{\frac{u(z)}{2} + \tfrac{1}{2} + \frac{u(z)}{2}\cos\left[2(\theta-\phi_m+\phi_a)\right]\right\}\cos\left[2n(\theta-\phi_m+\phi_a+\tfrac{1}{2}\phi_\rho)\right]$$

$$= \frac{\sqrt{k}}{2(1+kz^2)^{3/2}}\exp\left\{-h^2 - \frac{a^2}{4\sigma_1^2} + \frac{u(z)}{2}\right\}$$

$$\times\left\{\left[u(z)+1\right]I_o\left[\rho(z)\right] + u(z)I_1\left[\rho(z)\right]\cos\left[\phi_\rho(z)\right]\right\} \tag{A-25}$$

with

$$\rho^2 = \left(\frac{u(z)}{2} - \frac{a^2}{4\sigma_1^2}\cos 2\phi_b\right)^2 + \left(\frac{a^2}{4\sigma_1^2}\sin 2\phi_b\right)^2$$

and

$$\tan(\phi_\rho) = \frac{a^2}{4\sigma_1^2}\sin 2\phi_b \Bigg/ \left[\frac{u(z)}{2} - \frac{a^2}{4\sigma_1^2}\cos 2\phi_b\right] \Bigg\}. \qquad \text{(A-26)}$$

The resultant expression, then, for the FM detector output pdf is

$$p_5(z) = \frac{\sqrt{k}}{(1+kz^2)^{3/2}} \exp\left\{\frac{u(z)}{2} - h^2 - \frac{a^2}{4\sigma_1^2}\right\} \qquad \text{(A-27)}$$

$$\times\left\{\left[\frac{1+u(z)}{2}\right] I_0[\rho(z)] + \frac{u(z)}{2\rho(z)}\left[\frac{u(z)}{2} - \frac{a^2\cos 2\phi_b}{4\sigma_1^2}\right] I_1[\rho(z)]\right\}$$

where u(z) is given by (A-24).

Major Case

For $\dot{A} = 0$, (A-27) reduces to

$$p_5(z) = \frac{\sqrt{k}}{2}(1+kz^2)^{-3/2}\exp\left\{-\frac{h^2}{2}\left[1 + \frac{k(z-m)^2}{1+kz^2}\right]\right\} \qquad \text{(A-28)}$$

$$\times\left\{\left[1+h^2\frac{(1+mkz)^2}{1+kz^2}\right] I_0\left[\frac{h^2}{2}\left(\frac{1-m^2k+2mkz}{1+kz^2}\right)\right] + h^2\frac{(1+mkz)^2}{1+kz^2} I_1\left[\frac{h^2}{2}\left(\frac{1-m^2k+2mkz}{1+kz^2}\right)\right]\right\}$$

with the alternate expression (related to a Taylor's series expansion)

$$p_5(z) = \sqrt{\frac{k}{\pi}} e^{-h^2} (1+kz^2)^{-3/2}$$

$$\times \sum_{n=0}^{\infty} \frac{(h^2)^n}{(n!)^2} \frac{(1+mkz)^{2n}}{(1+kz^2)^n} \Gamma(n+\tfrac{3}{2})\, {}_1F_1\left(n+\tfrac{1}{2};\ n+1;\ -m^2kh^2\right). \qquad \text{(A-29)}$$

Unless the effect of (incidental) amplitude modulation is being studied, this case is sufficiently general for most purposes. If the detector model itself is to be studied in more detail, one can consult the appropriate chapters in Middleton's book [3].

Further specializations of (A-28) and (A-29) are the following subcases:

(a) For no signal (A=0),

$$p_5(z|A=0) = \frac{\sqrt{k}}{2}(1+kz^2)^{-3/2}. \tag{A-30}$$

(b) For no modulation (m=0), from (17) and (20)

$$p_5(z|m=0) = \frac{\sqrt{k}}{2} e^{-h^2}(1+kz^2)^{-3/2}\ {}_1F_1\left(3/2;1;\frac{h^2}{1+kz^2}\right) \tag{A-31}$$

$$= \frac{\sqrt{k}}{2}(1+kz^2)^{-3/2}\exp\left\{-\frac{h^2}{2}\left(\frac{1+2kz^2}{1+kz^2}\right)\right\}$$

$$\times\left\{\left(1+\frac{h^2}{1+kz^2}\right)I_o\left[\frac{h^2/2}{1+kz^2}\right]+\frac{h^2}{1+kz^2}I_1\left[\frac{h^2/2}{1+kz^2}\right]\right\}. \tag{A-32}$$

In the next section, the mean value is calculated to be

$$\bar{z} = m(1 - e^{-h^2}); \tag{A-33}$$

as the carrier SNR (≡CNR) increases, the mean approaches the noiseless case, as expected. In Figure A-1, this effect is demonstrated numerically for constant (frequency shift) modulation--that is, when $m = 2\pi f_d$; the bandwidth b was selected such that $m\sqrt{k} = 1$ ($b = f_d\sqrt{3}$). Also, the figure displays the pdf of the scaled variable $v = z/f_d$, so that asymptotically the mean approaches 2π.

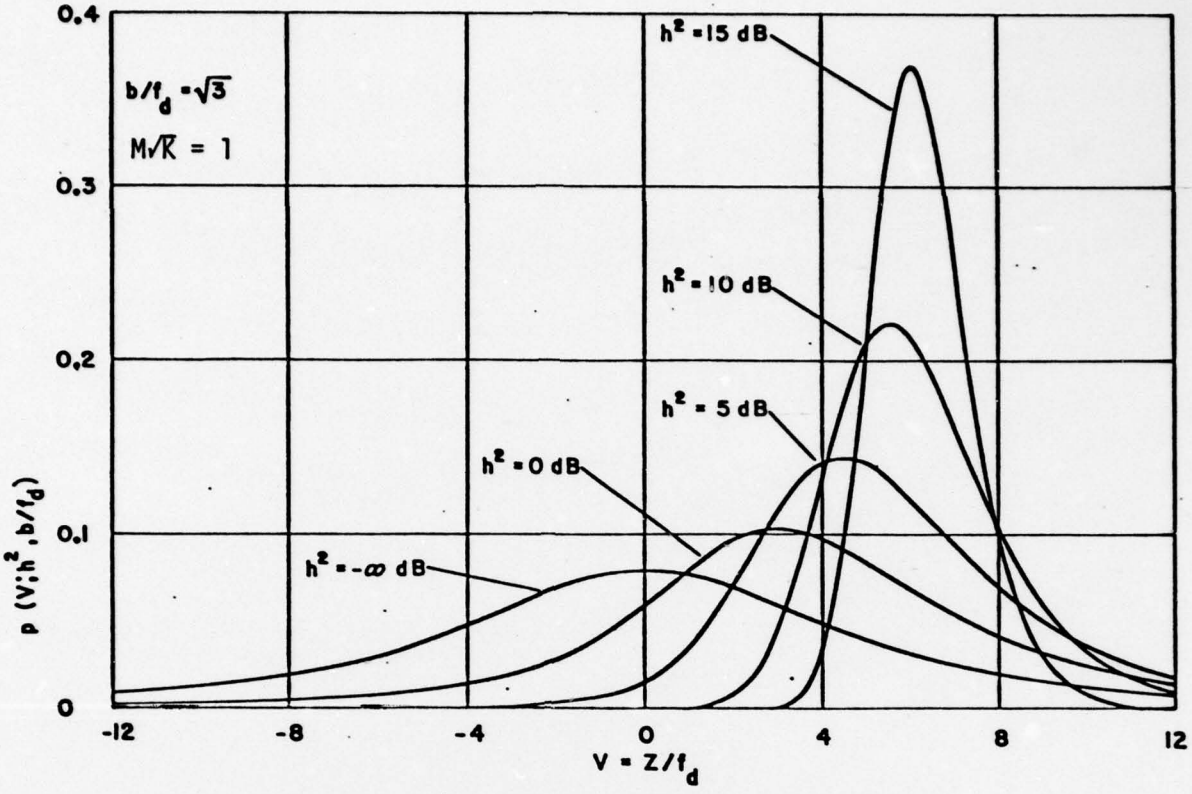

FIGURE A-1, FM DETECTOR OUTPUT pdf, CNR VARIED

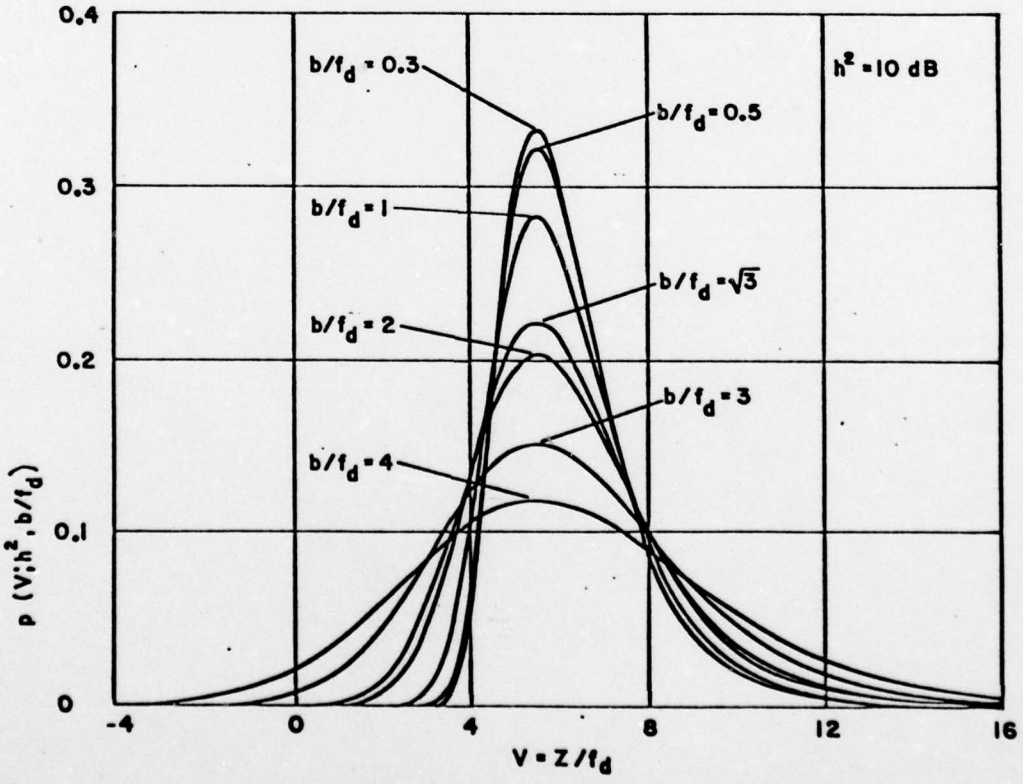

FIGURE A-2, FM DETECTOR OUTPUT pdf, BANDWIDTH VARIED

Another effect we anticipate is that, as the bandwidth of the post-limiter filter (b) is decreased, the output SNR decreases. Also, for fixed b, if the modulation or frequency shift f_d increases, the effective output SNR should increase. Both these effects are evident in Figure A-2.

B. Calculation of the Mean Value.

The mean value of the FM channel output for a given value of the modulation m is obtained from (A-29) by

$$E\{z;m\} = \sqrt{\frac{k}{\pi}}\, e^{-h^2} \sum_{n=0}^{\infty} \frac{h^{2n}}{n!n!}\, \Gamma(n+3/2)\, {}_1F_1(n+1/2;n+1;-m^2kh^2)$$

$$\times \int_{-\infty}^{\infty} dz\, \frac{z(1+mkz)^{2n}}{(1+kz^2)^{n+3/2}}\,, \qquad \text{(B-1)}$$

where the integral equals

$$\frac{1}{k}\int_{-\infty}^{\infty} \frac{dx(1+m\sqrt{k}x)^{2n}}{(1+x^2)^{n+3/2}} = \frac{1}{2k}\sum_{r=0}^{2n}\binom{2n}{r}(m\sqrt{k})^r \int_{-\pi/2}^{\pi/2} d\theta(\cos\theta)^{2n-r}(\sin\theta)^{r+1}$$

$$= \frac{1}{k}\sum_{r=0}^{n-1}\binom{2n}{2r+1}(m\sqrt{k})^{2r+1}\int_0^{\pi/2} d\theta(\cos\theta)^{2n-2r-1}(\sin\theta)^{2r+2}$$

$$= \frac{1}{k}\sum_{r=0}^{n-1}\binom{2n}{2r+1}(m\sqrt{k})^{2r+1} B(n-r,r+3/2). \qquad \text{(B-2)}$$

Here $B(x,y) = \Gamma(x)\Gamma(y)/\Gamma(x+y)$ is the beta function:

$$B(n-r,r+3/2) \equiv \frac{\Gamma(n-r)\Gamma(r+3/2)}{\Gamma(n+3/2)} \qquad \text{(B-3)}$$

Substituting (B-3) in (B-2) yields

$$\frac{1}{k}\frac{n!\,\Gamma(n+1/2)\sqrt{\pi}}{\Gamma(n+3/2)}\sum_{r=0}^{n-1}\frac{(m\sqrt{k})^{2r+1}}{r!\,\Gamma(n-r+1/2)} \tag{B-4}$$

With this expression for the integral, (B-1) becomes

$$E\{z;m\} = \frac{1}{\sqrt{k}}e^{-h^2}\sum_{n=0}^{\infty}\frac{h^{2n}}{n!}\,\Gamma(n+1/2)\,{}_1F_1(n+1/2;n+1;-m^2kh^2)$$

$$\times\sum_{r=0}^{n-1}\frac{(m\sqrt{k})^{2r+1}}{r!\,\Gamma(n-r+1/2)}$$

$$= \frac{1}{\sqrt{k}}e^{-h^2}\sum_{n=0}^{\infty}\sum_{r=0}^{\infty}\frac{(h^2)^{n+r+1}}{(n+r+1)!}\,\Gamma(n+r+3/2)\,{}_1F_1(n+r+3/2;n+r+2;-m^2kh^2)$$

$$\times\frac{(m\sqrt{k})^{2r+1}}{r!\,\Gamma(n+3/2)} \tag{B-5}$$

in which was used the progression

$$\sum_{n=0}^{\infty}\sum_{r=0}^{n-1}f(n,r) = \sum_{n=r+1}^{\infty}\sum_{r=0}^{\infty}f(n,r) = \sum_{n=0}^{\infty}\sum_{r=0}^{\infty}f(n+r+1,r). \tag{B-6}$$

Now, the summation over the index r may be recognized as a Taylor's series:

$$\sum_{r=0}^{\infty}\frac{(h^2m^2k)^r}{r!}\,\frac{(n+3/2)_r}{(n+2)_r}\,{}_1F_1(n+3/2+r;n+2+r;-m^2kh^2)$$

$$= {}_1F_1(n+3/2;n+2;m^2kh^2-m^2kh^2) \equiv 1. \tag{B-7}$$

This fortunately simplifies (B-5) to

$$E\{z;m\} = m\,e^{-h^2}\sum_{n=0}^{\infty}\frac{(h^2)^{n+1}}{(n+1)!} = m(1-e^{-h^2}). \tag{B-8}$$

C. Filter Integrals. The transition from equations (27) to (28) in the text can be shown as follows. The integral is

$$I = \int_0^T d\nu \int_0^T d\tau\, h(\nu)h(\tau)R_x(\tau-\nu), \tag{C-1}$$

in which $h(\nu)$ is a filter impulse response and $R_x(\tau)$ is a correlation function. Since $R_x(\tau)$ is even, there is a symmetry about the line $\tau=\nu$; thus rotating the coordinates ν,τ by 45^0 gives

$$I = 2\int_0^T d\nu \int_\nu^T d\tau\, h(\nu)h(\tau)R_x(\tau-\nu)$$

$$= 2\int_0^{T/\sqrt{2}} d\nu' R_x(-\nu'\sqrt{2}) \int_{\nu'}^{T\sqrt{2}-\nu'} d\tau' h\left(\frac{\tau'-\nu'}{\sqrt{2}}\right) h\left(\frac{\tau'+\nu'}{\sqrt{2}}\right). \tag{C-2}$$

Making use again of the even-ness of $R_x(\tau)$ and rescaling the variables results in

$$I = 2\int_0^T dv\, R_x(v) \int_0^{T-v} du\, h(u)h(u+v)$$

$$= 2\int_0^T dv\, R_x(v)g(v) \tag{C-3}$$

where $g(v)$ is the filter autocorrelation function for the case of $h(t)=0$, $t<0$ and $t>T$:

$$g(v) = \int_{-\infty}^{\infty} du\, h(u)h(u+v) = \int_0^{T-v} du\, h(u)h(u+v). \tag{C-4}$$

A corollary to this result occurs for $R_x(\tau) \equiv 1$:

$$\left\{\int_0^T d\nu\, h(\nu)\right\}^2 = \int_0^T d\nu \int_0^T d\tau\, h(\nu)h(\tau) = 2\int_0^T dv\, g(v). \qquad \text{(C-5)}.$$

For the various filters given in (16)-(18), we have ($\tau>0$)

$$\int_0^T dt\, h_1(t)=1,\ g_1(\tau) = \frac{1}{T}\left[1 - \frac{\tau}{T}\right]; \qquad \text{(C-6)}$$

$$\int_0^T dt\, h_2(t) = 1-e^{-T/RC},\ g_2(\tau) = \frac{e^{-\tau/RC}}{2RC}\left[1 - e^{-2(T-\tau)/RC}\right] \qquad \text{(C-7)}$$

and

$$\int_0^T dt\, h_3(t) = 1 - e^{-\omega_b T/\sqrt{2}}\left[\sin(\omega_b T/\sqrt{2}) + \cos(\omega_b T/\sqrt{2})\right]$$

$$g_3(\tau) = \frac{\omega_b}{\sqrt{8}}\left\{e^{-\omega_b \tau/\sqrt{2}}\left[\sin(\omega_b \tau/\sqrt{2}) + \cos(\omega_b T/\sqrt{2})\right]\right. \qquad \text{(C-8)}$$

$$\left. + e^{-\omega_b(2T-\tau)/\sqrt{2}}\left[\cos(\omega_b(2T-\tau)/\sqrt{2}) - \sin(\omega_b(2T-\tau)/\sqrt{2}) - 2\cos(\omega_b \tau/\sqrt{2})\right]\right\}.$$

REFERENCES

1. J. S. Lee Associates, Inc., "Some Analytical results obtained during the current period under contract N00014-77-C-0056," presented to Probability and Statistics Program office, ONR, 21 July 1978.

2. J. L. Lawson and G. E. Uhlenbeck, Threshold Signals, McGraw-Hill, New York, 1950.

3. D. Middleton, Introduction to Statistical Communication Theory, McGraw-Hill, New York, 1960.

4. P. C. Jain, "Error probabilities in binary angle modulation," IEEE Transactions on Information Theory, IT-20, pp 36-42 (January 1974).

5. Gradshteyn and Ryzhik, Table of Integrals, Series, and Products, Academic Press, New York, 1965.

6. H. Osawa, N. Morinaga, and T. Namekawa, "Output signal-to-noise ratios of FM correlation systems," IEEE Transactions on Information Theory, IT-17, pp 32-36 (January 1971).

7. M. C. Austin, "Wide-band frequency-shift keyed receiver performance in the presence of intersymbol interference," IEEE Transaction on Communications (concise paper), pp 453-458 (April 1975).

DISTRIBUTION LIST

	Copies
Statistics and Probability Program (Code 436) Office of Naval Research Arlington, VA 22217	3
Defense Documentation Center Cameron Station Alexandria, VA 22314	12
Office of Naval Research New York Area Office 715 Broadway - 5th Floor New York, New York 10003	1
Commanding Officer Office of Naval Research Branch Office Attn: D. A.L. Powell Building 114, Section D 666 Summer Street Boston, MA 02210	1
Commanding Officer Office of Naval Research Branch Office Attn: Director for Science 536 South Clark Street Chicago, Illinois 60605	1
Commanding Officer Office of Naval Research Branch Office Attn: Dr. Richard Lau 1030 East Green Street Pasadena, CA 91101	1
ARI Field Unit-USAREUR Attn: Library c/o ODCSPER HQ USAREUR & 7th Army APO New York 09403	1
Naval Underwater Systems Center Attn: Dr. Derrill J. Bordelon Code 21 Newport, Rhode Island 02840	1
Library, Code 1424 Naval Postgraduate School Monterey, California 93940	1
Technical Information Division Naval Research Laboratory Washington, DC 20375	1
Office of Naval Research San Francisco Area Office One Hallidie Plaza - Suite 601 San Francisco, CA 94102	1
Office of Naval Research Scientific Liaison Group Attn: Scientific Director American Embassy - Tokyo APO San Francisco 96503	1
Applied Mathematics Laboratory David Taylor Naval Ship Research and Development Center Attn: Mr. G. H. Gleissner Bethesda, Maryland 20084	1
Commandant of the Marine Corps (Code AX) Attn: Dr. A.L. Slafkosky Scientific Advisor Washington, DC 20380	1
Director National Security Agency Attn: Mr. Stahly and Dr. Maar (R51) Fort Meade, MD 20755	2
Navy Library National Space Technology Laboratory Attn: Navy Librarian Bay St. Louis, MS 39522	1
U.S. Army Research Office P.O. Box 12211 Attn: Dr. J. Chandra Research Triangle Park, NC 27706	1
Naval Sea Systems Command (NSEA 03F) Attn: Miss B. S. Orleans Crystal Plaza #6 Arlington, VA 20360	1
Office of the Director Bureau of The Census Attn: Mr. H. Nisselson Federal Building 3 Washington, DC 20233	1
OASD (I&L), Pentagon Attn: Mr. Charles S. Smith Washington, DC 20301	1

DISTRIBUTION LIST CON'T

	Copies
Col. B. E. Clark, USMC Code 100M Office of Naval Research Arlington, VA 22217	1
Library Naval Ocean Systems Center San Diego, CA 92152	1
Professor G. S. Watson Department of Statistics Princeton University Princeton, NJ 08540	1
Professor T. W. Anderson Department of Statistics Stanford University Stanford, CA 94305	1
Professor M. R. Leadbetter Department of Statistics University of North Carolina Chapel Hill, NC 27514	1
Professor M. Rosenblatt Department of Mathematics University of California, San Diego La Jolla, CA 92093	1
Professor E. Parzen Department of Statistics Texas A&M University College Station, Texas 77840	1
Professor W. R. Schucany Department of Statistics Southern Methodist University Dallas, Texas 75275	1
Professor P.A.W. Lewis Department of Operations Research Naval Postgraduate School Monterey, CA 93940	1
Professor E. Masry Department of Applied Physics and Information Science University of California La Jolla, CA 92093	1
Professor N. J. Bershad School of Engineering University of California Irvine, California 92664	1
Professor I. Rubin School of Engineering and Applied Science University of California Los Angeles, CA 90024	1
Professor L. L. Scharf, Jr. Department of Electrical Engineering Colorado State University Fort Collins, CO 80521	1
Professor R. W. Madsen Department of Statistics University of Missouri Columbia, Missouri 65201	1

DISTRIBUTION LIST CON'T

	Copies
Professor M. J. Hinich Department of Economics Virginia Polytechnic Institute and State University Blacksburg, Virginia 24061	1
Naval Coastal Systems Center Code 741 Attn: Mr. C.M. Bennett Panama City, FL 32401	1
J. S. Lee Associates, Inc. 2001 Jefferson Davis Highway Suite 201 Arlington, VA 22202	1
Naval Electronic Systems Command (NELEX 320) National Center No. 1 Arlington, Virginia 20360	1
Professor D. P. Gaver Department of Operations Research Naval Postgraduate School Monterey, California 93940	1
Professor Bernard Widrow Stanford Electronics Laboratories Stanford University Stanford, California 94305	1
Dr. M. J. Fischer Defense Communications Agency Defense Communications Engineering Center 1860 Wiehle Avenue Reston, Virginia 22090	1
Professor S. M. Ross College of Engineering University of California Berkeley, CA 94720	1

	Copies
Professor L. A. Aroian Institute of Administration and Management Union College Schenectady, New York 12308	1
Professor Grace Wahba Department of Statistics University of Wisconsin Madison, Wisconsin 53706	1
Professor Donald W. Tufts Department of Electrical Engineering University of Rhode Island Kingston, Rhode Island 02881	1
Professor S. C. Schwartz Department of Electrical Engineering and Computer Science Princeton University Princeton, New Jersey 08540	1
Professor Charles R. Baker Department of Statistics University of North Carolina Chapel Hill, NC 27514	1
Mr. David Siegel Code 210T Office of Naval Research Arlington, VA 22217	1
Professor Balram S. Rajput Department of Mathematics University of Tennessee Knoxville, Tennessee 37916	1